

A Novel Benchmark for Few-Shot Semantic Segmentation in the Era of Foundation Models

Reda Bensaid^{1,2}, Vincent Gripon¹, François Leduc-Primeau², Lukas Mauch³,
Ghouthi Boukli Hacene^{3,4}, and Fabien Cardinaux³

¹ IMT Atlantique, Brest, France
name.surname@imt-atlantique.fr

² Polytechnique Montréal, Montreal, Canada

{reda-2.bensaid, francois.leduc-primeau}@polymtl.ca

³ Sony Europe, B.V. Stuttgart Laboratory 1, Germany
name.surname@sony.com

⁴ Mila, Montreal, Canada

Abstract. In recent years, the rapid evolution of computer vision has seen the emergence of various foundation models, each tailored to specific data types and tasks. In this study, we explore the adaptation of these models for few-shot semantic segmentation. Specifically, we conduct a comprehensive comparative analysis of four prominent foundation models: DINO V2, Segment Anything, CLIP, Masked AutoEncoders, and of a straightforward ResNet50 pre-trained on the COCO dataset. We also include 5 adaptation methods, ranging from linear probing to fine tuning. Our findings show that DINO V2 outperforms other models by a large margin, across various datasets and adaptation methods. On the other hand, adaptation methods provide little discrepancy in the obtained results, suggesting that a simple linear probing can compete with advanced, more computationally intensive, alternatives ⁵

Keywords: Deep Learning · Foundation models · Semantic Segmentation · Few-Shot Learning

1 Introduction

Semantic segmentation, the task of pixel-level object classification within images, plays a pivotal role in computer vision applications [22]. In recent years, few-shot semantic segmentation has emerged as a challenging yet essential frontier [31]. This paradigm seeks to adapt models to novel object classes with minimal labeled data. A standard pipeline for few-shot semantic segmentation typically comprises two key components: a pretrained feature extractor, often derived from a vision foundation model, and an adapter method [2]. This setup leverages the knowledge embedded within the feature extractor and adapts it to the limited labeled data without the risk of overfitting. While extensive discussions regarding the selection of feature extractors for few-shot classification have been

⁵ Code to be released at: https://github.com/RedaBensaidDS/Foundation_FewShot

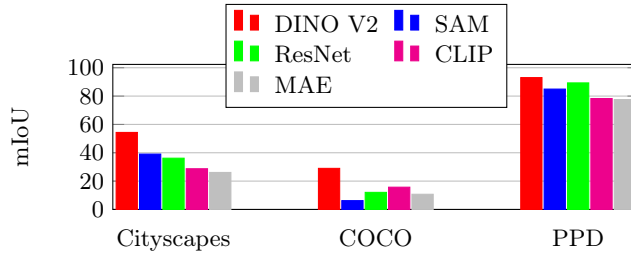


Fig. 1: mIoU of various pretrained models when adapted to 3 different 1-shot segmentation tasks (only best performance achieved out of 5 tested methods is displayed).

well-documented [21], the question of the optimal feature extractor for few-shot semantic segmentation remains largely unaddressed in the literature.

The primary objective of our research is to investigate which vision foundation model yields the most effective few-shot semantic segmentation pipeline. We are the first, to our knowledge, to systematically test the adaptation capabilities of renowned foundation models to this specific challenge. To this end, we introduce a novel benchmark, constructed using three widely-recognized semantic segmentation datasets, and systematically evaluate multiple adaptation methods. The four foundation models under consideration are DINO V2 [27], Segment Anything (SAM) [15], CLIP [28], and a Masked AutoEncoder [12] pre-trained on ImageNet-1K. Our experimental results consistently demonstrate the superior performance of DINO V2 across various datasets.

In summary, from our study we claim the following key contributions:

- We introduce a standardized benchmark for the evaluation of few-shot semantic segmentation in the context of vision foundation models.
- Based on this benchmark, we conduct a comprehensive comparison of five feature extractors (four foundation models) and five adaptation methods.
- We conduct extensive experiments to better understand the elementary contribution of foundation models design (e.g. type of architecture, size, training dataset) onto the obtained performance.

Our findings indicate that DINO V2 consistently outperforms all other models across multiple datasets and adaptation methods, with SAM yielding competitive results, particularly on some datasets (Figure 1). Additionally, we find that simple and efficient adaptation methods produce results comparable to more complex counterparts, showing yet again the importance of feature extraction on top of that of downstream segmentation heads. We anticipate that our research will assist in selecting appropriate solutions for few-shot semantic segmentation tasks and contribute to the rigorous benchmarking of this evolving field.

2 Benchmark

2.1 Task Formulation

In accordance with the established terminology of few-shot classification [32], our benchmark revolves around the concept of a support set \mathcal{S} and a query set \mathcal{Q} . The support set \mathcal{S} comprises a limited number of images, each accompanied by their corresponding ground truth segmentation. These support images are employed for the *training* or *calibration* of a generic semantic segmentation model. In contrast, the query set \mathcal{Q} serves as the evaluation dataset on which we compute the mean Intersection-over-Union (mIoU). In practical applications, \mathcal{Q} is typically not available and is utilized exclusively for benchmarking purposes.

To compute the mIoU, we calculate the Intersection-over-Union (IoU) for each class i and then average these values:

$$\text{mIoU} = \frac{1}{n} \sum_{i=1}^n \frac{\text{TP}_i}{\text{TP}_i + \text{FP}_i + \text{FN}_i},$$

where n represents the total number of classes or objects, TP_i is the true positive count for class i , FP_i is the false positive count for class i , and FN_i is the false negative count for class i . One noteworthy distinction from few-shot classification is that individual images typically contain instances from various classes of interest. As such, it is challenging to define tasks in the k -shot manner, where each class is associated with exactly k elements in the support set.

In our proposed framework, we introduce a more practical approach. We define a k -shot segmentation task as one in which the support set \mathcal{S} contains *at least* k instances of each class. Using our proposed sampling protocol described in the next subsection, in a scenario involving a total of n classes, a k -shot task mandates the inclusion of precisely nk unique images within the support set.

2.2 Benchmark Generation

To construct few-shot tasks from readily available semantic segmentation datasets, we employ the following sampling procedure:

1. Initialize an empty support set, denoted as $\mathcal{S} = \emptyset$.
2. For each class i (excl. the background class) within the chosen dataset \mathcal{D} , we compile a list of all training images that contain at least one instance of that class, resulting in $\mathcal{D}_i = \{\text{image} \in \mathcal{D} \mid \text{image contains instances of class } i\}$.
3. Following an arbitrary order of classes, we randomly select k images from \mathcal{D}_i without replacement to be incorporated into the support set \mathcal{S} . We ensure that images are only selected once.
4. In the event that there are insufficient remaining images for a particular class i , we restart from Step 1. It is important to note that this reset condition did not occur in the course of our experiments.

3 Datasets

In constructing our proposed benchmark, we have selected three prominent semantic segmentation datasets, each offering unique characteristics:

Cityscapes [3] is a large scale dataset on semantic understanding of urban scene streets. It contains 2,975 images for training, 500 for validation and 1,525 for testing. It is annotated using 19 classes (such as “car”, “road”, “building”) and has input resolution 1024x2048.

COCO (Microsoft Common Objects in Context) [19] is a large scale dataset used for multiple tasks including semantic segmentation. The 2017 release contains 118k images for training, 5k for validation and 41k for testing. It is annotated using 80 classes (such as “person”, “bicycle”, “elephant”). Images in COCO often exhibit varying input resolutions, commonly falling between 400 and 640 pixels for both width and height.

PPD (PLANT PHENOTYPING DATASETS) [23] is a small dataset used for multiple tasks including plant segmentation (foreground to background) and leaf segmentation (multi-instance segmentation). We focus in our work on the plant segmentation task, where the dataset contains 783 images and 2 classes (foreground and background). Typical input resolutions for PPD images hover around 500 pixels for both width and height. Contrary to the two other datasets, we considered the background to be a class of its own for benchmark generation, meaning that a 1-shot problem would contain 2 support images.

4 Backbones and Adaptation Methods

In this section, we introduce the methodologies that form the basis of our comparative study. Drawing from existing literature on both few-shot classification [21] and few-shot semantic segmentation [2], we have identified that the majority of methods rely on a combination of two fundamental components.

The first essential component is a *pretrained model*, typically a transformer or a convnet. Notably, these pretrained models are not necessarily designed specifically for semantic segmentation but offer valuable preexisting knowledge.

The second critical component is an *adaptation method*, a mechanism devised to tailor the knowledge encoded within the pretrained model for effective utilization in the specific task of interest.

Next, we provide comprehensive details on the specific models and adaptation methods that constitute the experimental foundation of our study.

4.1 Pretrained Models

In our study, we investigate five pretrained models, each offering unique characteristics and advantages (see also summary in Table 13):

MAE (Masked AutoEncoder) [12] is a model pretrained on ImageNet-1K [6] using a self-supervised technique involving masking portions of input images and reconstructing them using partial tokens from the unmasked segments.

It comprises a Vision Transformer (ViT) [7] component that maps observed image regions into latent representations and a decoder for image reconstruction. Previous research [12] has demonstrated MAE’s effectiveness in transfer learning for segmentation tasks, particularly in semantic segmentation.

SAM (Segment Anything Model) [15] is a recent foundation model for segmentation, pretrained on the SA-1B dataset, which includes 11 million images and 1 billion segmentation masks. SAM exhibits robust generalization capabilities across a broad range of segmentation tasks. It utilizes a Vision Transformer (ViT) [7] initialized with a MAE [12], a prompt encoder, and a mask decoder. SAM’s image encoder generates embeddings from input images, which are subsequently employed by the mask decoder in conjunction with the prompt encoder. While SAM’s mask decoder outputs class-agnostic masks intended for segmenting instances or objects at various granularities, our specific task focuses exclusively on the encoder’s role as a feature extractor and does not require prompts.

DINO v2 [27] is a foundational vision model trained using the self-supervised technique [1] called DINO. This method consists in having two networks with the same architecture, namely the teacher and the student. The student parameters are learned by minimizing a loss measuring the discrepancy between teacher and student outputs learning a “local to global” correspondence where the student processes global and local views of the image while the teacher only processes the global views. The teacher is built with an exponential moving average of past iteration of the student. The model comprises a ViT trained on a diverse range of datasets, including notable semantic segmentation datasets like Cityscapes [3], ADE20k [42, 43], and Pascal VOC 2012 [8]. DINO v2 has previously been evaluated on (not few-shot) semantic segmentation datasets in [27], utilizing the frozen backbone and a simple segmentation decoder.

CLIP (Contrastive Language-Image Pre-training) [28] is a model that consists of two encoders: a vision encoder and a text encoder. These encoders are jointly trained using a contrastive loss to align embeddings of images with their corresponding captions. The model is pretrained on a private dataset of 400 million (image, text) pairs and has gained significant attention for its utility in zero-shot classification on downstream tasks. In our study, we exclusively leverage the ViT version of the visual encoder component of CLIP.

FCN (Fully Convolutional Network) [20] is a conventional convolutional architecture extensively used for semantic segmentation tasks. It comprises an encoder and a decoder, with the former composed of convolutional layers and the latter incorporating deconvolutional layers. In our configuration, the encoder is based on ResNet50 [13] and is pretrained on a subset of COCO, specifically using the 20 classes shared with the Pascal VOC dataset. We incorporate FCN as a convolution-only benchmark for comparison.

4.2 Methods

We then consider five adaptation methods in our study, ranging from linear probing methods to partial fine-tuning and full fine-tuning methods:

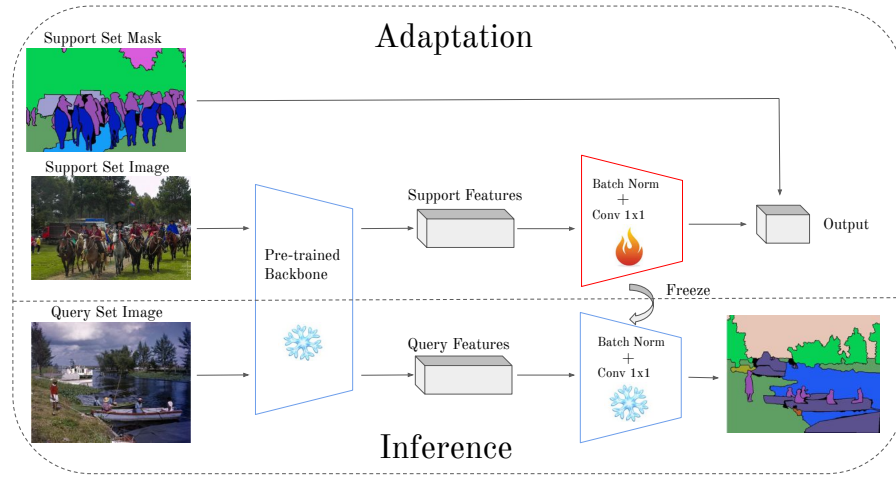


Fig. 2: The pipeline of the Linear method: we freeze the backbone and train the shallow decoder on the support set, and then we test the encoder+decoder on the query set.

Linear: A common approach [27,33] consists in freezing the pretrained backbone and adding a segmentation head, called *decoder*, consisting of a batch normalization layer followed by a convolutional 1x1 layer. Figure 2 illustrates the overall pipeline for this linear adaptation method.

Multilayer: It has been shown in [27] and [38] that using a concatenation of multiple layers from the pretrained model can boost performance in downstream tasks. We thus propose to use a linear method on the concatenation of the last 4 blocks of the pretrained model.

Singular Value Fine-tuning [34] (SVF): The SVF method decomposes parameters into three matrices using Singular Value Decomposition (SVD) and fine-tunes only the singular values diagonal matrix while keeping the rest frozen. In [34], this approach demonstrated promising results in few-shot semantic segmentation tasks, showcasing its ability to specialize the pretrained model without overfitting. In our study, we initially apply the linear method and then proceed to fine-tune the singular values of the encoder alongside the decoder parameters.

Low-Rank Adaptation [14] (LoRA): In this approach, we maintain the pretrained backbone’s frozen state and introduce low-rank trainable adapters, as described in [14]. Similarly to the SVF method, LoRA enables tuning only a limited number of parameters. Our procedure begins with training the decoder using the linear method and then introduces LoRA adapters to the encoder. Subsequently, we fine-tune both the adapters and decoder parameters.

Fine-tuning: The fine-tuning method, a straightforward yet effective approach, involves fine-tuning the entire pretrained model. This method has demonstrated state-of-the-art performance in few-shot classification [21]. However, it is susceptible to overfitting due to the limited number of training samples compared to the typically extensive parameter pool in the considered encoders.

5 Experiments

5.1 Training Procedure

To ensure the reproducibility of our results, we conducted all experiments with three fixed random seeds and computed the mean Intersection-over-Union (mIoU) across these runs. For preprocessing, we followed the approach outlined in [10]. This involved random horizontal flipping, random scaling of the shorter side within the range of [400, 1600] while preserving the aspect ratio, and random cropping to a size of 1024x1024. We applied a subset of RandAug [4] operations, including auto contrast, equalize, rotate, color, contrast, brightness, and sharpness. Subsequently, all images were resized to 1024x1024 resolution, except for CLIP and MAE, which accept input sizes of 224x224. We acknowledge that the resolution variation, depending on the considered model, may introduce some analysis challenges but was an unavoidable aspect of our setup. For the learning rate, we employed the poly learning rate scheduler with a power of 0.9 for the linear and multilayer methods. Specifically, we used a learning rate of 0.2 for Cityscapes, 0.05 for COCO, and 0.001 for PPD. For fine-tuning methods (SVF, LoRA, and fine-tune), we did a grid search across models and datasets with values including 10^{-2} , 10^{-3} , 10^{-4} , 10^{-5} , and 10^{-6} to determine the one yielding the best average performance. Linear and multilayer methods were trained with a batch size of 4. For the Fine-tuning, SVF, and LoRA methods, we initiated the training with the linear method and subsequently performed fine-tuning with the reduced batch size of 2, addressing memory limitations. Training duration extended to 200 epochs for Cityscapes and PPD, and 100 epochs for COCO. The query set consisted of the standard validation sets for Cityscapes and COCO. For PPD, given the absence of a conventional split, we performed a fixed 50/50 random split into training and validation sets. Our models were trained on a combination of NVIDIA A6000 and NVIDIA RTX3090 GPUs. Runtime varied across datasets and models, ranging from approximately 30 minutes per run for MAE, CLIP, and ResNet on Cityscapes to approximately 4 hours per run for DINO V2 on COCO. For the size of the models, we chose the base version of the vision transformers, leading to a 89M parameters model for SAM and 86M for DINO V2, CLIP and MAE. For the FCN we chose a ResNet50 as an encoder, leading to a 23M parameters model.

5.2 What Works The Best?

First, we aim to identify the optimal combination of pretrained models and adaptation methods based on mIoU. Table 1 presents the average performance on the three considered datasets for all possible combinations of pretrained models and adaptation methods, along with their standard deviation, in the context of 1-shot problems. Several conclusions can be drawn:

- DINO V2 consistently outperforms all other models across various settings. This superiority is especially notable on Cityscapes and COCO, where DINO

Table 1: mIoU averaged over our three considered datasets in 1-shot few-shot semantic segmentation. Bold numbers correspond to the best performance across feature extractors and underline numbers to the best performance across adaptation methods.

	Linear	Multilayer	SVF	LoRA	Fine-tuning
SAM	40.66±09.00	43.36±02.52	41.84±16.83	43.10±03.38	42.35±09.91
DINO V2	54.78±03.09	53.51±03.10	57.77±04.20	57.67±02.50	57.21±04.04
CLIP	35.88±10.90	39.57±07.29	<u>40.90±13.93</u>	38.23±04.50	38.69±10.20
MAE	35.50±10.16	36.65±07.38	<u>37.76±08.08</u>	36.37±04.22	36.46±10.28
FCN-ResNet50	37.78±04.17	<u>44.08±02.16</u>	43.40±08.63	41.45±03.70	39.63±06.49

V2 surpasses other models by a significant margin (see Appendix Table 9 for the detailed results). It is worth noting that Cityscapes is included in the training images of DINO V2, although it only had access to the images and not their associated segmentation masks.

- SAM encoder exhibits strong performance on average. It outperforms CLIP, MAE, and ResNet on both Cityscapes and PPD. However, it yields comparatively poor results on COCO (refer to Appendix Table 9). This difference is likely attributed to our decision to retain the SAM image encoder while discarding the original mask decoder.
- The multilayer method outperforms the linear approach for most models, indicating that including earlier feature maps, which are more locally focused [7, 29], provides the decoder with greater segmentation flexibility. Furthermore, it exhibits a lower standard deviation, indicating greater stability across the different runs of our proposed benchmark.
- Despite variations in the number of trainable parameters (less than 1% for LoRA, around 2% for SVF, and 100% for finetune), the finetuning methods (SVF, LoRA, and Full Fine-tuning) yield comparable results between them.

We then vary the number of shots to 2, 5 and 10. Table 2 shows the consistency of the results with 1-shot, where:

- DINO V2 outperforms other models by a big margin.
- SAM still yields strong performance on average, but performs poorly on COCO (refer to appendix Tables 10, 11, 12).
- The multilayer method outperforms the linear approach for most models.
- Fine-tuning methods yield comparable results.

In addition, we can see that:

- DINO V2 scales better than other models with more shots.
- Fine-tuning scales better than LoRA and SVF and gives better results on average on the 10-shot setting, this is due to the fact that we suffer less from over-fitting when having more shots.

Table 2: mIoU averaged over our three considered datasets in k -shot semantic segmentation for $k \in \{2, 5, 10\}$. Bold numbers correspond to the best performance across extractors and underline numbers to the best performance across adaptation methods.

		Linear	Multilayer	SVF	LoRA	Fine-tuning
2-shot	SAM	42.30±03.72	46.78±01.61	46.56±01.96	45.78±02.94	45.73±02.16
	DINO V2	61.20±00.29	59.21±00.83	64.10±00.83	63.73±01.28	64.35±00.33
	CLIP	39.08±03.45	43.46±00.70	<u>45.59±01.94</u>	42.72±02.97	35.68±07.11
	MAE	36.90±04.15	38.73±02.39	40.36±03.83	<u>40.37±04.27</u>	39.15±03.50
	FCN-ResNet50	40.98±01.96	47.36±00.85	48.66±00.92	<u>46.55±02.36</u>	<u>48.81±00.32</u>
5-shot	SAM	46.55±00.82	51.73±00.21	49.93±00.21	51.57±00.24	<u>52.24±00.29</u>
	DINO V2	66.47±00.60	65.89±00.63	68.64±00.88	67.54±00.20	68.82±01.40
	CLIP	46.30±00.29	48.67±00.61	<u>51.56±00.22</u>	49.00±00.39	43.60±00.76
	MAE	44.36±00.23	45.02±00.15	46.20±00.92	<u>47.02±00.16</u>	46.68±00.34
	FCN-ResNet50	47.02±00.48	49.70±00.27	<u>51.58±00.03</u>	51.40±00.28	51.51±00.26
10-shot	SAM	47.79±00.39	54.26±00.11	51.41±00.29	54.20±00.37	<u>55.20±00.48</u>
	DINO V2	69.86±00.23	69.95±00.12	69.97±00.69	69.25±00.25	71.07±01.35
	CLIP	50.14±00.41	52.49±00.41	<u>53.64±00.77</u>	51.92±00.41	47.62±03.36
	MAE	47.56±00.41	47.97±00.28	46.73±00.17	42.94±03.07	<u>48.63±00.30</u>
	FCN-ResNet50	48.69±00.69	51.98±00.25	<u>53.04±00.31</u>	53.02±00.25	52.86±00.55

5.3 Practical Considerations

Previous values were obtained by selecting the best learning rates on the validation sets. Instead, here we study the effect of transferring the learning rate from a dataset to another one on the mIoU. The learning rate values we explored are 10^{-2} , 10^{-3} , 10^{-4} , 10^{-5} and 10^{-6} . Table 3 shows the drop of mIoU when we train a pair (model, method) on dataset A with the best learning rate for dataset B. We can see that the learning rate is relatively consistent between the 3 datasets and especially between Cityscapes and COCO for a given model and a given method. even though the optimal values are not exactly the same between these datasets, the variation of performance is low and applying the optimal learning of one dataset on the other does not cause a big drop of performance, so we argue that these values could serve as a good baseline for a new unseen dataset. The higher drops occur when we either take the optimal learning rate for PPD or when we test an optimal learning rate of Cityscapes or COCO on PPD. This is mainly due to the fact that the support set of PPD is significantly smaller than that of the other considered datasets.

5.4 Individual Factors

In the next series of experiments, we study the effect of various elements that could influence the performance of the models. Namely, these include the model size, the underlying architecture, the pretrained dataset and the pretraining method. By studying these individual components, we seek to provide a more granular understanding of what drives model performance.

Table 3: Drop in mIoU when using the best learning rate corresponding to the dataset on the line (source) when training on the dataset on the column (target), instead of using the target validation set to find the best learning rate.

		SVF			LoRA			Fine-tuning		
		Cityscapes	COCO	PPD	Cityscapes	COCO	PPD	Cityscapes	COCO	PPD
SAM	Cityscapes	-	0	0	-	0	0	-	2.72	22.83
	COCO	0	-	0	0	-	0	0.94	-	3.01
	PPD	0	0	-	0	0	-	3.38	3.83	-
DINO	Cityscapes	-	0	0	-	0	2.31	-	0	15.62
	COCO	0	-	0	0	-	2.00	0	-	26.3
	PPD	0	0	-	0.88	0.88	-	1.17	1.17	-
CLIP	Cityscapes	-	0	0.40	-	0.52	0.52	-	0	0
	COCO	0	-	1.09	0.24	-	0	0	-	0
	PPD	1.91	1.91	-	1.53	0	-	0	0	-
MAE	Cityscapes	-	0.19	0.19	-	0.54	0.54	-	0.12	0
	COCO	0.28	-	0	0.87	-	0	0.65	-	0.65
	PPD	1.41	0	-	1.47	0	-	0	1.53	-
ResNet	Cityscapes	-	1.07	0.23	-	0.82	0	-	0.56	0
	COCO	0.88	-	4.07	0.66	-	0.66	1.55	-	1.55
	PPD	8.46	18.01	-	0	7.85	-	0	12.13	-

Input Resolution. We explore how input resolution impacts model performance, a critical factor given our training setup. Specifically, CLIP and MAE were trained at a resolution of 224x224, while other models were trained with a higher resolution of 1024x1024. This discrepancy is due to the fixed input size requirements of CLIP and MAE’s positional embeddings. To address this, we adapted the positional embeddings matrix for variable resolutions, a common practice for ViT models. Our findings, illustrated in Figure 3, reveal a divergence in performance trends: increasing resolution degrades results for CLIP and MAE but improves them for DINO V2. This can be attributed to DINO V2’s training across multiple resolutions, unlike CLIP and MAE. Consequently, this suggests using 1024x1024 input images on DINO V2 whereas 224x224 input images on CLIP and MAE is fair for performance comparison.

Model Size. Table 4 demonstrates that a larger model size does not translate to a big boost of performance. Specifically, for SAM and DINO V2 with the linear method, the base model (ViT-B) yields, on average, competitive performance, despite having 3 times less parameters than the (ViT-L) models. In the case of ResNet, moving from ResNet-50 to ResNet-101 shows a performance boost, though the increase is modest. For the LoRA method, fine-tuning of a subset of parameters of the encoder yields better performance with bigger models. These observations partially accounts for the performance discrepancy between SAM, DINO V2, and ResNet50, highlighting the influence of model size differences.

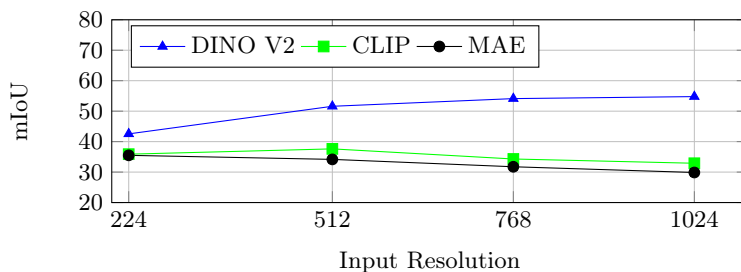


Fig. 3: Impact of the input resolution on the obtained mIoU.

Table 4: Effect of model size on mIoU.

	Linear			LoRA		
	Cityscapes	COCO	PPD	Cityscapes	COCO	PPD
SAM (ViT-B)	35.72±01.50	03.13±00.09	83.14±10.36	38.50±00.12	05.85±00.13	84.94±10.11
SAM (ViT-L)	35.00±01.29	03.43±00.07	72.95±09.05	40.70±00.45	07.31±00.37	79.14±10.75
SAM (ViT-H)	34.64±01.36	03.38±00.11	83.34±04.02	40.78±00.57	07.46±00.29	85.73±08.42
DINO V2 (ViT-S)	41.16±02.39	20.62±00.38	87.99±05.58	44.75±00.71	22.72±00.71	86.55±06.08
DINO V2 (ViT-B)	48.80±01.82	23.24±00.38	92.31±01.84	54.35±01.55	28.99±01.33	89.67±06.43
DINO V2 (ViT-L)	49.36±01.61	23.50±00.33	87.87±07.30	54.79±00.64	31.54±00.81	87.46±07.97
FCN-ResNet50	32.39±01.79	10.08±00.32	70.86±05.91	35.74±01.41	11.71±00.24	76.91±10.29
FCN-ResNet101	32.97±01.76	10.94±00.16	69.70±12.98	29.38±07.03	12.23±00.57	81.79±11.40

Training Dataset. To examine the impact of the training dataset on model performance, we compared DINO V1 and DINO V2, noting that the primary distinction between them lies in their training datasets. DINO V1 was trained on ImageNet-1K, whereas DINO V2 utilized a much larger dataset comprising 142M curated and uncurated images. It is important to mention that another difference between the two models is the employed loss function, although the focus of this analysis is primarily on the effect of dataset size and composition. Table 5 illustrates that DINO V2 significantly surpasses DINO V1 in performance, with DINO V1 exhibiting notably weak results on the COCO dataset. Showing that having a bigger training dataset is beneficial for the downstream task performance on few-shot semantic segmentation.

Table 5: Effect of the training dataset on mIoU

	Linear			LoRA		
	Cityscapes	COCO	PPD	Cityscapes	COCO	PPD
DINO V1	29.03±01.08	05.92±00.39	82.14±10.04	32.53±00.97	06.89±00.44	82.99±09.35
DINO V2	48.80±01.82	23.24±00.38	92.31±01.84	54.35±01.55	28.99±01.33	89.67±06.43

Architecture. To assess the influence of model architecture, we analyzed the performance differences between DINO V1 (ViT-S) and its ResNet-50 variant, alongside comparing the CLIP (ViT-B) version against the CLIP ResNet-50 version. It is noteworthy that for CLIP, the ViT-B model is larger than its ResNet counterpart, an aspect previously discussed in terms of model size impact. According to Table 6, ViT architectures demonstrate a clear performance advantage over their ResNet equivalents. This trend underscores the potential superiority of ViT models in adapting to various tasks.

Table 6: Effect of model architecture on mIoU

	Linear			LoRA		
	Cityscapes	COCO	PPD	Cityscapes	COCO	PPD
DINO V1 (ViT-S)	26.61±00.53	04.86±00.23	81.86±08.19	29.90±00.95	05.82±00.34	79.70±09.03
DINO V1 (ResNet-50)	23.51±01.40	03.42±00.05	58.98±00.61	26.98±01.28	03.78±00.04	77.35±10.50
CLIP (ViT-B)	23.83±01.51	11.32±00.31	72.49±10.78	27.95±01.62	13.62±00.78	73.13±11.70
CLIP (ResNet-101)	20.22±01.57	02.61±00.06	69.00±06.03	08.96±00.11	00.91±00.03	67.40±11.91

Training Method. To investigate the effect of different self-supervised learning (SSL) methods on model performance, we conducted a comparison between DINO V1 and MAE. Both models were trained on the same dataset (ImageNet-1K), and share identical architecture and size (ViT-B with 86M parameters), making the SSL method the primary variable. The comparison in Table 7 reveals that DINO V1 surpasses MAE on the Cityscapes and PPD datasets, whereas MAE demonstrates superior performance on COCO. This mixed outcome indicates that there is no definitive answer as to which SSL training approach offers the best adaptability for few-shot segmentation tasks.

Table 7: Effect of the training method on mIoU

	Linear			LoRA		
	Cityscapes	COCO	PPD	Cityscapes	COCO	PPD
DINO V1	29.03±01.08	05.92±00.39	82.14±10.04	32.53±00.97	06.89±00.44	82.99±09.35
MAE	23.63±00.89	08.54±00.46	74.34±10.88	26.10±00.26	10.13±00.42	72.87±12.83

Registers. In the study by [5], it is demonstrated that DINO V2, unlike its predecessor DINO V1, presents artifacts within its feature maps. This phenomenon is attributed to the presence of tokens with unusually high norms, which are integral to the model’s internal computations. To address this issue, the authors introduced a modified version of DINO V2, incorporating additional tokens termed

“Registers” during the training phase, which are subsequently omitted during inference. As evidenced in Table 8, this innovative approach significantly enhances DINO V2’s performance on the COCO dataset, showcasing the potential benefits of Registers during training for few-shot segmentation tasks.

Table 8: Effect of training with registers on mIoU

	Linear			LoRA		
	Cityscapes	COCO	PPD	Cityscapes	COCO	PPD
DINO V2 w/o Registers	48.80±01.82	23.24±00.38	92.31±01.84	54.35±01.55	28.99±01.33	89.67±06.43
DINO V2 w/ Registers	48.06±02.46	27.42±00.72	91.58±02.41	54.08±00.44	34.02±02.26	91.03±02.03

5.5 In Depth Analysis

In this section, we delve into the reasons behind SAM’s poor performance on the COCO dataset, exploring two main hypotheses:

- **Decoder Limitations:** The primary suspect for SAM’s subpar performance is the dependency of the image encoder on the prompt encoder and the mask decoder. To address this, we replaced the original mask decoder with a transformer decoder, as detailed in [15], modifying it for few-shot semantic segmentation following the inspiration from [41]. We introduced a constant prompt to the decoder, altering tokens to produce an N -class depth map rather than binary masks, and eliminated the IoU score output branch. We experimented with two mask decoder configurations, one with a Conv Transpose module and another where we upsampled the output through interpolation, while initializing remaining modules with pretrained weights. Despite these adjustments, this approach was outperformed by a simpler linear decoding method by up to 5% mIoU, likely due to the challenges of training a complex decoder in a Few-shot scenario.
- **Mask Distribution Bias:** Another investigated issue was the mask distribution bias in COCO towards image centers, unlike the distribution in the SA-1B dataset used for SAM, highlighted in [15], where masks are more evenly distributed. We attempted to mitigate this bias with various preprocessing techniques (RandomCrop, CenterCrop, dividing each image into four smaller images); however, these modifications did not enhance our results.

These findings shed light on the specific challenges faced by SAM in adapting to the COCO dataset and highlight the complexities involved in optimizing for few-shot semantic segmentation tasks.

6 Related Work

In this section, we discuss related work in the literature in few-shot classification and semantic segmentation.

6.1 Few-Shot Classification

Few-shot classification initially focused on in-domain tasks, with benchmarks involving dataset splitting into training, validation, and fake few-shot task generation for evaluation [9,30,32,37]. The introduction of Meta-dataset [36] marked a shift towards the cross-domain setting, where the dataset used for model training differs from the tasks evaluated later, aligning with more realistic scenarios. More recently, the field has embraced the use of foundation models, adapting them to few-shot tasks. Notably, benchmarks such as those in [44] explore the application of CLIP [28] to 11 downstream tasks.

Methodologically, diverse approaches have emerged, ranging from hallucination-based [11,16] to meta-learning [9,24,25,40]. Straightforward methods have also demonstrated effectiveness [17,18,35]. Recent surveys, such as [21], suggest that optimal approaches often involve simple finetuning atop competitive pretrained models, augmented with an additional linear layer. This observation motivates the methods introduced in our paper.

6.2 Semantic Segmentation and Few-Shot Semantic Segmentation

Few-shot semantic segmentation is not a recent topic. Earlier works, such as [31] and [26], explored multiple benchmarks, including PASCAL-5ⁱ and COCO-20ⁱ, reminiscent of in-domain benchmarks used in few-shot classification. Subsequent research ventured into using pretrained models on ImageNet [39], resembling the Meta-dataset approach in few-shot classification. Notably, most of these studies assumed binary labelling for the few-shots, emphasizing a single object of interest in the available shot images, considering all other objects as background.

In contrast, our approach considers that the provided few-shots are fully labelled, and we leverage pretrained foundation models, not limited to those trained solely on ImageNet. This approach aligns more closely with contemporary industrial requirements, focusing on the utilization of the most efficient available models, without specific explicit restrictions.

7 Conclusion

In conclusion, DINO V2 emerges as the top-performing backbone model, consistently outperforming other foundation models. While SAM exhibits strong overall results, it presents unexpected limitations on certain datasets. Surprisingly, our experiments underscore the competitive advantages of straightforward methods such as simple linear segmentation heads trained on the few given shots, challenging the necessity of complex procedures.

This work not only presents a comparison of techniques but also a practical benchmark. We hope this benchmark will contribute to improving few-shot semantic segmentation methods and will provide a solid ground for comparison.

References

1. Caron, M., Touvron, H., Misra, I., Jégou, H., Mairal, J., Bojanowski, P., Joulin, A.: Emerging properties in self-supervised vision transformers (2021) [5](#)
2. Catalano, N., Matteucci, M.: Few shot semantic segmentation: a review of methodologies and open challenges (2023) [1](#), [4](#)
3. Cordts, M., Omran, M., Ramos, S., Rehfeld, T., Enzweiler, M., Benenson, R., Franke, U., Roth, S., Schiele, B.: The cityscapes dataset for semantic urban scene understanding (2016) [4](#), [5](#)
4. Cubuk, E.D., Zoph, B., Shlens, J., Le, Q.V.: Randaugment: Practical automated data augmentation with a reduced search space (2019) [7](#)
5. Darcet, T., Oquab, M., Mairal, J., Bojanowski, P.: Vision transformers need registers (2023) [12](#)
6. Deng, J., Dong, W., Socher, R., Li, L.J., Li, K., Fei-Fei, L.: Imagenet: A large-scale hierarchical image database. In: 2009 IEEE Conference on Computer Vision and Pattern Recognition. pp. 248–255 (2009). <https://doi.org/10.1109/CVPR.2009.5206848> [4](#)
7. Dosovitskiy, A., Beyer, L., Kolesnikov, A., Weissenborn, D., Zhai, X., Unterthiner, T., Dehghani, M., Minderer, M., Heigold, G., Gelly, S., Uszkoreit, J., Houlsby, N.: An image is worth 16x16 words: Transformers for image recognition at scale (2021) [5](#), [8](#)
8. Everingham, M., Van Gool, L., Williams, C.K.I., Winn, J., Zisserman, A.: The PASCAL Visual Object Classes Challenge 2012 (VOC2012) Results. <http://www.pascal-network.org/challenges/VOC/voc2012/workshop/index.html> [5](#)
9. Finn, C., Abbeel, P., Levine, S.: Model-agnostic meta-learning for fast adaptation of deep networks (2017) [14](#)
10. Gao, R.: Rethinking dilated convolution for real-time semantic segmentation (2023) [7](#)
11. Hariharan, B., Girshick, R.: Low-shot visual recognition by shrinking and hallucinating features (2017) [14](#)
12. He, K., Chen, X., Xie, S., Li, Y., Dollár, P., Girshick, R.: Masked autoencoders are scalable vision learners (2021) [2](#), [4](#), [5](#)
13. He, K., Zhang, X., Ren, S., Sun, J.: Deep residual learning for image recognition (2015) [5](#)
14. Hu, E.J., Shen, Y., Wallis, P., Allen-Zhu, Z., Li, Y., Wang, S., Wang, L., Chen, W.: Lora: Low-rank adaptation of large language models (2021) [6](#)
15. Kirillov, A., Mintun, E., Ravi, N., Mao, H., Rolland, C., Gustafson, L., Xiao, T., Whitehead, S., Berg, A.C., Lo, W.Y., Dollár, P., Girshick, R.: Segment anything (2023) [2](#), [5](#), [13](#)
16. Li, K., Zhang, Y., Li, K., Fu, Y.: Adversarial feature hallucination networks for few-shot learning (2020) [14](#)
17. Li, W.H., Liu, X., Bilen, H.: Universal representation learning from multiple domains for few-shot classification (2021) [14](#)
18. Li, W.H., Liu, X., Bilen, H.: Cross-domain few-shot learning with task-specific adapters (2022) [14](#)
19. Lin, T.Y., Maire, M., Belongie, S., Bourdev, L., Girshick, R., Hays, J., Perona, P., Ramanan, D., Zitnick, C.L., Dollár, P.: Microsoft coco: Common objects in context (2015) [4](#)

20. Long, J., Shelhamer, E., Darrell, T.: Fully convolutional networks for semantic segmentation (2015) 5
21. Luo, X., Wu, H., Zhang, J., Gao, L., Xu, J., Song, J.: A closer look at few-shot classification again (2023) 2, 4, 6, 14
22. Minaee, S., Boykov, Y., Porikli, F., Plaza, A., Kehtarnavaz, N., Terzopoulos, D.: Image segmentation using deep learning: A survey (2020) 1
23. Minervini, M., Fischbach, A., Scharr, H., Tsaftaris, S.A.: Finely-grained annotated datasets for image-based plant phenotyping. *Pattern Recognition Letters* pp. 1–10 (2015) 4
24. Munkhdalai, T., Yu, H.: Meta networks (2017) 14
25. Munkhdalai, T., Yuan, X., Mehri, S., Trischler, A.: Rapid adaptation with conditionally shifted neurons (2018) 14
26. Nguyen, K., Todorovic, S.: Feature weighting and boosting for few-shot segmentation (2019) 14
27. Oquab, M., Darcet, T., Moutakanni, T., Vo, H., Szafraniec, M., Khalidov, V., Fernandez, P., Haziza, D., Massa, F., El-Nouby, A., Assran, M., Ballas, N., Galuba, W., Howes, R., Huang, P.Y., Li, S.W., Misra, I., Rabbat, M., Sharma, V., Synnaeve, G., Xu, H., Jegou, H., Mairal, J., Labatut, P., Joulin, A., Bojanowski, P.: Dinov2: Learning robust visual features without supervision (2023) 2, 5, 6
28. Radford, A., Kim, J.W., Hallacy, C., Ramesh, A., Goh, G., Agarwal, S., Sastry, G., Askell, A., Mishkin, P., Clark, J., Krueger, G., Sutskever, I.: Learning transferable visual models from natural language supervision (2021) 2, 5, 14
29. Raghu, M., Unterthiner, T., Kornblith, S., Zhang, C., Dosovitskiy, A.: Do vision transformers see like convolutional neural networks? (2022) 8
30. Ravi, S., Larochelle, H.: Optimization as a model for few-shot learning. In: *International Conference on Learning Representations* (2017), <https://openreview.net/forum?id=rJY0-Kc1l> 14
31. Shaban, A., Bansal, S., Liu, Z., Essa, I., Boots, B.: One-shot learning for semantic segmentation (2017) 1, 14
32. Snell, J., Swersky, K., Zemel, R.S.: Prototypical networks for few-shot learning (2017) 3, 14
33. Strudel, R., Garcia, R., Laptev, I., Schmid, C.: Segmenter: Transformer for semantic segmentation (2021) 6
34. Sun, Y., Chen, Q., He, X., Wang, J., Feng, H., Han, J., Ding, E., Cheng, J., Li, Z., Wang, J.: Singular value fine-tuning: Few-shot segmentation requires few-parameters fine-tuning (2022) 6
35. Tian, Y., Wang, Y., Krishnan, D., Tenenbaum, J.B., Isola, P.: Rethinking few-shot image classification: a good embedding is all you need? (2020) 14
36. Triantafillou, E., Zhu, T., Dumoulin, V., Lamblin, P., Evcı, U., Xu, K., Goroshin, R., Gelada, C., Swersky, K., Manzagol, P.A., Larochelle, H.: Meta-dataset: A dataset of datasets for learning to learn from few examples (2020) 14
37. Vinyals, O., Blundell, C., Lillicrap, T., Kavukcuoglu, K., Wierstra, D.: Matching networks for one shot learning (2017) 14
38. Xie, E., Wang, W., Yu, Z., Anandkumar, A., Alvarez, J.M., Luo, P.: Segformer: Simple and efficient design for semantic segmentation with transformers (2021) 6
39. Yang, L., Zhuo, W., Qi, L., Shi, Y., Gao, Y.: Mining latent classes for few-shot segmentation (2021) 14
40. Zhang, C., Ding, H., Lin, G., Li, R., Wang, C., Shen, C.: Meta navigator: Search for a good adaptation policy for few-shot learning (2021) 14
41. Zhong, Z., Tang, Z., He, T., Fang, H., Yuan, C.: Convolution meets lora: Parameter efficient finetuning for segment anything model (2024) 13

42. Zhou, B., Zhao, H., Puig, X., Fidler, S., Barriuso, A., Torralla, A.: Scene parsing through ade20k dataset. In: 2017 IEEE Conference on Computer Vision and Pattern Recognition (CVPR). pp. 5122–5130 (2017). <https://doi.org/10.1109/CVPR.2017.544> 5
43. Zhou, B., Zhao, H., Puig, X., Xiao, T., Fidler, S., Barriuso, A., Torralla, A.: Semantic understanding of scenes through the ade20k dataset (2018) 5
44. Zhou, K., Yang, J., Loy, C.C., Liu, Z.: Learning to prompt for vision-language models. *International Journal of Computer Vision* **130**(9), 2337–2348 (Jul 2022). <https://doi.org/10.1007/s11263-022-01653-1>, <http://dx.doi.org/10.1007/s11263-022-01653-1> 14

8 Appendix

8.1 Detailed Results for Every Dataset

We can see in Tables 9, 10, 11, 12 the detailed results on the 3 datasets separately:

- The range of performance on the 3 datasets is different mainly due to the varying size and number of classes. On PPD, we only have 2 classes making the task easier but the training is more unstable due to the restricted number of training examples, since we only have 2 images in our support set. This leads to a bigger standard deviation in PPD compared to COCO and Cityscapes since the choice of these 2 images is crucial and the images are different between the 3 folders constituting the dataset.
- SAM image encoder performance is poor on COCO compared to other models even though it outperformed all the models except DINO V2 in the other 2 datasets. This is probably due to the fact that we isolated the image encoder (the adaptation of the whole SAM model to prompt free Few-Shot Semantic Segmentation is left to future work).

8.2 Model Comparison Summary

Table 13 summarizes the main components of the different models used in our study, we discuss the importance of each component (Architecture, Size, Pre-training Dataset, Pre-training Method) in 5.4.

8.3 Impact on the Number of Shots

We can see in Fig. 4 that for SVF, the different models scale similarly and that models are still outperformed by DINO V2 even when more shots are available. We can see in Fig. 5 that for DINO V2, the gap between the models tends to be smaller the more we increase the number of shots. Also, full fine-tuning scales a better than other methods because we are less prone to overfitting, leading to the conclusion that it is better to choose the full fine-tuning method when more shots are available. Yet it is not crucial since the full fine tuning is time and memory expensive compared to the other methods, and a simple method Linear adaptation can give good performance with a minor drop in performance.

Table 9: Detailed results of mIoU on our three considered datasets in 1-shot semantic segmentation.

		Linear	Multilayer	SVF	LoRA	Fine-tuning
Cityscapes	SAM	35.72±01.50	39.06±01.97	38.90±00.48	38.50±00.12	38.14±00.40
	DINO V2	48.80±01.82	46.77±02.80	51.96±01.37	54.35±01.55	50.87±01.25
	CLIP	23.83±01.51	26.10±02.01	<u>28.72±01.06</u>	27.95±01.62	27.74±01.38
	MAE	23.63±00.89	23.81±00.76	25.88±00.32	26.10±00.26	25.07±00.64
	FCN-ResNet50	32.39±01.79	34.12±02.01	36.14±01.19	35.74±01.41	<u>36.17±01.41</u>
COCO	SAM	03.13±00.09	06.21±00.32	05.31±00.09	05.85±00.13	05.16±00.31
	DINO V2	23.24±00.38	20.92±00.19	28.30±00.77	28.99±01.33	28.15±01.24
	CLIP	11.32±00.31	14.47±00.29	15.70±00.71	13.62±00.78	15.13±00.91
	MAE	8.54±00.46	08.60±00.45	<u>10.52±00.45</u>	10.13±00.42	10.71±00.57
	FCN-ResNet50	10.08±00.32	08.82±00.88	<u>12.05±00.33</u>	11.71±00.24	<u>11.88±00.38</u>
PPD	SAM	83.14±10.36	84.82±00.43	81.32±17.07	84.94±10.11	83.75±10.01
	DINO V2	92.31±01.84	92.85±01.76	93.05±02.57	89.67±06.43	92.61±02.10
	CLIP	72.49±10.78	78.14±06.81	<u>78.28±12.63</u>	73.13±11.70	73.19±08.69
	MAE	74.34±10.88	77.54±07.95	76.90±07.95	72.87±12.83	73.62±10.59
	FCN-ResNet50	70.86±05.91	<u>89.31±01.88</u>	82.01±08.04	76.91±10.29	70.84±06.15

Table 10: Detailed results of mIoU on our three considered datasets in 2-shot semantic segmentation.

		Linear	Multilayer	SVF	LoRA	Fine-tuning
Cityscapes	SAM	38.84±00.38	42.71±00.24	40.24±01.18	40.62±00.29	40.63±00.77
	DINO V2	56.54±00.75	53.36±00.09	58.21±01.00	58.84±01.75	58.60±00.57
	CLIP	25.19±01.05	28.96±01.62	<u>30.85±00.42</u>	30.53±01.19	19.29±04.90
	MAE	24.15±00.32	24.88±00.51	27.68±00.21	<u>27.92±00.51</u>	26.83±00.32
	FCN-ResNet50	36.40±00.57	37.89±00.45	<u>38.98±00.06</u>	38.34±00.28	38.97±00.33
COCO	SAM	04.45±00.03	09.30±00.43	07.92±00.22	08.82±00.31	08.99±00.47
	DINO V2	33.08±00.17	30.01±00.57	39.91±00.90	39.01±01.36	40.09±00.68
	CLIP	16.03±00.47	18.85±00.67	<u>22.33±00.46</u>	20.40±00.99	21.85±00.84
	MAE	12.20±00.69	12.26±00.66	15.30±00.27	15.26±00.34	<u>15.66±00.21</u>
	FCN-ResNet50	12.54±00.50	11.44±00.48	13.23±00.78	<u>13.42±00.81</u>	12.55±00.83
PPD	SAM	83.62±10.89	88.32±04.81	<u>91.51±05.99</u>	87.89±09.03	87.56±07.23
	DINO V2	93.96±01.44	94.24±02.03	94.17±01.68	93.33±02.18	94.35±00.86
	CLIP	76.01±10.95	82.58±03.02	<u>83.59±05.94</u>	77.21±09.11	65.92±15.61
	MAE	74.36±12.50	<u>79.05±07.61</u>	78.12±11.30	77.93±12.92	74.97±10.59
	FCN-ResNet50	74.01±05.93	92.74±02.02	93.76±02.01	87.88±06.22	94.91±00.59

Table 11: Detailed results of mIoU on our three considered datasets in 5-shot semantic segmentation.

		Linear	Multilayer	SVF	LoRA	Fine-tuning
Cityscapes	SAM	41.15±01.71	44.90±00.74	42.29±00.32	44.58±00.68	45.15±00.68
	DINO V2	59.71±02.30	59.22±02.16	61.22±01.97	61.69±01.37	62.88±01.74
	CLIP	28.70±01.20	31.21±01.62	<u>33.88±01.23</u>	33.23±00.78	13.40±01.31
	MAE	27.49±00.72	28.19±01.01	<u>30.67±00.91</u>	<u>30.92±00.96</u>	29.91±01.03
	FCN-ResNet50	37.68±00.97	39.85±00.13	42.42±00.17	42.80±00.43	<u>43.30±00.75</u>
COCO	SAM	05.92±00.17	14.01±00.05	11.89±00.72	14.30±00.45	14.92±00.76
	DINO V2	44.48±00.64	42.32±00.66	49.07±01.59	45.82±01.80	50.52±01.34
	CLIP	26.71±00.57	29.11±00.67	<u>31.85±00.15</u>	30.71±00.11	31.61±00.39
	MAE	19.20±00.52	19.27±00.44	<u>21.67±00.46</u>	22.80±00.40	<u>23.39±00.39</u>
	FCN-ResNet50	15.42±00.27	14.23±00.65	15.47±00.23	<u>15.94±00.16</u>	14.09±00.10
PPD	SAM	92.59±01.81	96.28±00.19	95.61±00.65	95.82±00.58	96.65±00.78
	DINO V2	95.21±00.35	<u>96.13±00.35</u>	95.62±00.47	95.11±00.39	93.06±03.70
	CLIP	83.48±01.12	85.68±00.43	<u>88.94±00.58</u>	83.07±01.68	85.76±01.16
	MAE	86.39±00.42	<u>87.61±00.31</u>	86.26±01.99	87.34±00.74	86.73±00.36
	FCN-ResNet50	87.97±00.79	95.02±01.11	96.84±00.15	95.45±00.65	97.13±0.02

Table 12: Detailed results of mIoU on our three considered datasets in 10-shot semantic segmentation.

		Linear	Multilayer	SVF	LoRA	Fine-tuning
Cityscapes	SAM	42.10±01.24	48.41±00.34	42.74±00.42	46.75±00.27	47.17±00.68
	DINO V2	63.19±00.23	63.64±00.64	63.38±00.45	63.87±00.46	66.24±00.49
	CLIP	32.44±01.32	34.83±00.82	<u>36.76±01.07</u>	36.50±01.17	21.83±10.21
	MAE	30.46±00.28	30.59±00.18	<u>32.63±00.75</u>	<u>32.99±00.45</u>	31.85±00.55
	FCN-ResNet50	40.63±00.66	43.20±00.38	45.12±00.53	45.56±00.62	45.63±01.38
COCO	SAM	07.13±00.25	17.81±00.33	15.02±00.31	19.36±00.74	21.32±00.49
	DINO V2	50.84±00.43	49.83±00.34	50.84±01.23	48.55±00.66	52.74±01.09
	CLIP	33.75±00.36	<u>36.45±00.53</u>	35.36±00.54	35.38±00.33	34.19±00.10
	MAE	25.38±00.22	25.88±00.29	20.96±00.54	08.84±11.26	<u>26.86±00.25</u>
	FCN-ResNet50	17.04±00.43	16.74±00.46	16.81±00.24	<u>17.15±00.21</u>	15.55±00.17
PPD	SAM	94.15±00.66	96.57±00.07	96.48±00.14	96.49±00.13	97.12±00.54
	DINO V2	95.55±00.15	96.38±00.24	95.67±00.53	95.32±00.41	94.24±02.64
	CLIP	84.24±00.51	86.18±00.27	<u>88.81±00.76</u>	83.37±00.74	86.84±00.39
	MAE	86.84±00.74	<u>87.44±00.48</u>	86.59±00.46	87.00±01.90	87.17±00.45
	FCN-ResNet50	88.40±01.72	96.01±00.28	97.18±00.20	96.34±00.16	97.39±00.11

Table 13: Summary of the main model elements.

	Architecture	Size	Dataset	Pre-training Method
SAM	ViT	89M	SA-1B	MAE + Prompt Segmentation
DINO V2	ViT	86M	142M image dataset	DINO (SSL with Knowledge Distillation)
CLIP	ViT	86M	400M of (image,text) pairs	image, text embedding alignment
MAE	ViT	86M	ImageNet-1K	Masking + Image reconstruction
FCN-ResNet50	CNN	23M	Subset of COCO	Semantic Segmentation

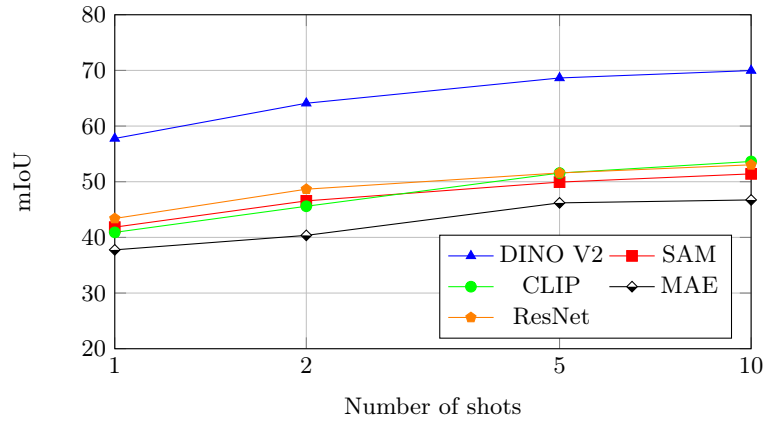


Fig. 4: Impact of the number of shots on mIoU for the SVF method.

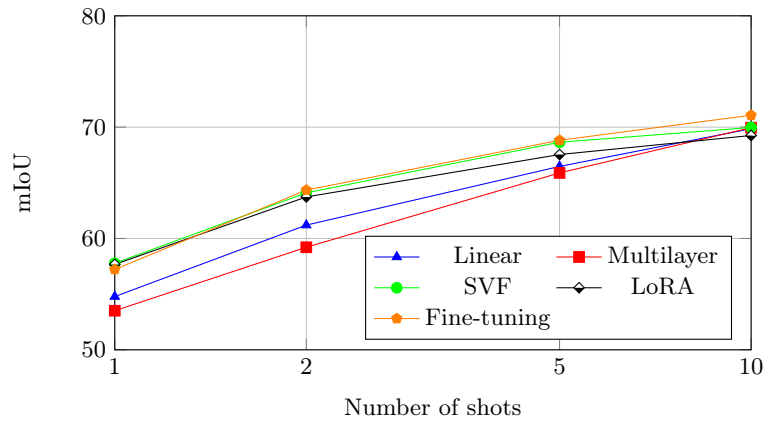


Fig. 5: Impact of the number of shots on mIoU for DINO V2.